REPORT DOCUMENTATION PAGE

Form Approved
OMB No. 0704-0188

1. AGENCY USE ONLY (Leave blank)	2. REPORT DATE	3. REPORT TYPE AND DATES COVERED
	10-31-95	FINAL TECHNICAL 10/1/02-12/31/05

4. TITLE AND SUBTITLE
Swept-Carrier Time-Domain Optical Memory
(F49620-92-J-0443)

5. FUNDING NUMBERS
61102F
2305/DS

6. AUTHOR(S)
Thomas W. Mossberg

7. PERFORMING ORGANIZATION NAME(S) AND ADDRESS(ES)
University of Oregon
Eugene OR 97403

c/o Research and Sponsored Programs

AFOSR-TR-95
0710

9. SPONSORING/MONITORING AGENCY NAME(S) AND ADDRESS(ES)
Department of the Air Force
Air Force Office of Scientific Reseasrch (AFMC) NE
AFOSR/~~PKBE~~
110 Duncan Avenue, Suite B115
Bolling AFB, DC 20332-0001

10. SPONSORING/MONITORING AGENCY REPORT NUMBER
F49620-92-J-0443

11. SUPPLEMENTARY NOTES
The view opinions and/or findings contained in this report are those of the author(s) and should not be construed as an official Department of the Air Force position, policy, or decision, unless so designated by other documentation.

12a. DISTRIBUTION/AVAILABILITY STATEMENT
Approved for public release; distribution unlimited

12b. DISTRIBUTION CODE

13. ABSTRACT *(Maximum 200 words)*

Results of a comprehensive study of spectral holography (the interaction of lasers with frequency-selective recording materials) is reported. New technologies, potentially capable of dramatically outperforming existing ones, have been identified and experimentally demonstrated. Impacted areas involve optical data storage, bit-rate conversion, and routing. The world's highest areal density x data bandwidth memory was demonstrated.

19951122 072

DTIC QUALITY INSPECTED 1

14. SUBJECT TERMS			15. NUMBER OF PAGES
Spectral Holeburning	Optical Routing	Bit-Rate Conversion	17
Optical Memory	Holography	Spectral Holography	16. PRICE CODE

17. SECURITY CLASSIFICATION OF REPORT	18. SECURITY CLASSIFICATION OF THIS PAGE	19. SECURITY CLASSIFICATION OF ABSTRACT	20. LIMITATION OF ABSTRACT
unclassified	UNC	UNC	UL

Table of Contents

Thomas W. Mossberg, P. I.
Department of Physics
University of Oregon

Executive Summary

(F49620-92-J-0443)

The objective of this AFOSR-funded project was to perform an exploratory experimental and theoretical study of the unique optical effects that arise through the interaction of temporally structured light beams with frequency-selective recording materials. This general subject area has, owing to the presence of fundamental analogies with existing phenomena, come to be known as spectral holography. Results obtained in the course of the funded research indicate that entirely new technologies supportive of computation and communication may be derived from spectral holographic processes identified and studied. In most cases, the spectral-holographic-based technologies examined have been found to possess performance limits far beyond those characteristic of established technologies. Spectral-holographic-based technologies investigated include ultra-high density and speed optical memory, ultrahigh speed optical routing, optical bit-rate conversion, and optical processing. Three of these processes were demonstrated for the very first time in the course of this project.

The storage of data at the highest (areal density) × (data bandwidth) product ever realized by optical or magnetic means (1.5×10^{17} bits/in^2-s) was demonstrated using the swept-carrier, time-domain, optical memory process. In the same experiments, an areal recording density of approximately 8 Gbits/in^2 or about an order of magnitude greater than current state-of-the-art magnetic or optical storage technologies was achieved. The areal storage density achieved was limited by laser tuning range and not fundamental process limits. Ultimate areal capacity of the specific storage material employed was estimated to be on the order of 100 Gbit/in^2. Theoretical analysis of spectral-holographic-based optical memories in general has revealed that areal densities in the Terabit/in^2 range are consistent with process limitations. Theoretical analysis of the swept-carrier memory has led to the development of a number of process variants that allow for its extremely simple implementation. These new variations of the swept-carrier memory process, involving heterodyne detection and single-sideband data storage, were experimentally demonstrated. Supportive of the swept-carrier memory studies, a highly monochromatic and frequency agile semiconductor diode laser system was developed. Based on commercial diode lasers, an external locking cavity, and electrooptic tuning, sub Megahertz linewidth and Gigahertz/μsec tuning rates were achieved.

An entirely new, spectral-holographic-based, approach to the spatial routing of optical data streams was discovered and demonstrated. In this routing scheme, optical signals incident along one direction are routed into diverse output directions based solely on address information encoded on their temporal profiles. This routing method, which involves entirely passive device response, may provide for extremely high bandwidth

routing capability.

Research conducted in the course of this grant has demonstrated the very substantial technological potential of optical processes based on spectral holographic interactions. Identification of new processes and potential applications has become routine. Barriers to immediate application of spectral holographic techniques are found to lie in the materials regime. Spectral storage capabilities of materials has not been extensively investigated. Currently, extreme spectral storage capacity is found only at low temperatures. The process development work completed in the course of the present grant provides a clear motivation to initiate an extensive materials evaluation program.

The funded research led to the publication (or pending publication) of seven articles in refereed scientific journals. Six of the publications appeared in the rapid publication journal of Optics Letters, while the other publication appeared in J. Opt. Soc. Am. B. One additional publication is in preparation. Two full-time Ph.D. students, an undergraduate, and a Post Doctoral Research Associate participated in the funded research. The funded research lead to a variety of invited talks at major conferences including the annual meeting of the Optical Society of America and, in fact, to the organization of symposia dedicated to this new field.

Thomas W. Mossberg, P. I.
Department of Physics
University of Oregon

Final Technical Report
(F49620-92-J-0443)

Introduction

Increases in the amount and rate of data passing through computer and communication systems over the last decades have been staggering. Impressively, existing storage, transmission, and processing technologies have accommodated this growth by evolving upward in capacity without fundamental changes in methodology. Looking to the future, one sees a continued rapid growth in demand for capacity. Problems loom because several important traditional technologies employed in data storage, processing, and transmission are approaching physics-limited maximum usable capacities. In the area of storage density, for example, diffraction-limited optical storage is already at its physics limits while magnetic storage soon will be. As fundamental process limits come into view, it is essential to seek new processes based on entirely different and perhaps novel principles that can accommodate performance levels *dramatically* beyond those currently attainable.

This Final Report describes the results of a program aimed at the investigation of a new class of optical processes based on the interaction of temporally and/or spatially complex light beams with frequency-selective optical recording materials. These processes may form the basis of a wide range of devices including ultrahigh speed and density optical memories, optical waveform processors, bit-rate converters, and temporal-waveform-controlled spatial routers. Performance levels expected are extreme. In the case of memory applications, for example, it may be possible to encode information at volume densities within a few orders of magnitude of the atomic density itself. Optical processing and routing functions become possible at multi Gigabit/sec data rates. All of the functions just mentioned derive from the unique potential of frequency-selective materials to record Fourier spectra of single or multiple complex time-domain optical waveforms, and to reconvert stored spectra or product spectra back into the time-domain for subsequent use.

Spatial Holography - Background

All applications of light are based on its interaction with materials - of various sorts and under various circumstances. Light does not measurably interact with itself. The range of light-matter interactions that are possible depends crucially on the characteristics of the physical material involved. Many materials have the characteristic that they respond locally to the intensity of light incident upon them through, for example, changes in optical absorptivity or index of refraction. Holography is based on the local spatial response of materials to imposed light intensity. In the holographic recording process, two simultaneous light beams are employed (see Figure 1a). The interference of these beams produces a spatial intensity variation containing detailed information on the spatial

Thomas W. Mossberg, P. I.
Department of Physics
University of Oregon

wavefronts of the beams. When one of the two beams is a simple plane wave (the reference beam) the intensity interference term simply represents the electric field of the other (object) beam. Since the holographic recording material is modified according to imposed intensity, the interference term and hence the electric field of a spatially complex (for example image carrying) object beam is recorded. In the holographic readout process (see Fig. 1b), material modifications introduced in the storage process modify the electric field of a readout optical beam so as to produce a signal beam whose field is identical to that of the object beam. Many variations on this basic three-beam holographic process are possible and have numerous technological applications.

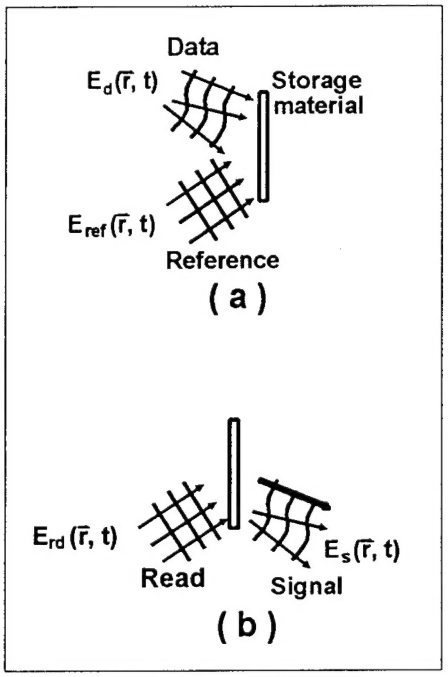

Figure 1. (a) Storage through interference. (b) Recall through filtering.

Spatial-Spectral Holography

Recently, another class of recording materials has been attracting increasing attention[1-6]. These materials exhibit a response that is local both spatially *and* spectrally. At a single spatial location, the recording material can respond independently at a multitude of different frequencies. Thus it can spectrally multiplex data at each spatial location.

Interaction of light beams with frequency-selective recording materials leads to a new class of phenomena which has come to be known as spectral holography (or spatial-spectral holography if both spatial and spectral recording is utilized). This designation is apt, because phenomena involved have direct parallels in spatial holography[7]. In spectral holography input beams need not be simultaneous and they may possess complex temporal structure. The storage material's ability to independently respond to separate frequencies at each spatial location, provides for the recording of the *temporal* structures of the input fields as well as their spatial structures.

These results have a simple analytic motivation. Assume that the storage material is a thin sheet and that only three input beams are involved. With three-beam effects, recording occurs (as in spatial holography) when the material is illuminated by two light beams (Fig. 1(a)), the data beam and the reference beam. The beams are of finite duration and need not be simultaneous. They may be temporally (and/or spatially) encoded with information. The recording material undergoes an absorptivity (or possibly an index) change in proportion to the optical energy fluence created at each spatial and spectral

Thomas W. Mossberg, P. I.
Department of Physics
University of Oregon

position by the data and reference beams. If $E_{ref}(\vec{r},t)$ and $E_d(\vec{r},t)$ represent the electric fields of the reference and data beams as they impinge on the storage material and the Fourier transforms

$$E_\epsilon(\vec{r},\nu)=\int_{-\infty}^{\infty} E_\epsilon(\vec{r},t)\, e^{-2\pi i\nu t}\, dt, \tag{1}$$

where ϵ specifies one of the laser fields, then the total optical energy fluence seen by the material as a function of spatial and spectral position is proportional to

$$|E_{tot}(\vec{r},\nu)|^2 = |E_{ref}(\vec{r},\nu)|^2 + |E_d(\vec{r},\nu)|^2 + \{E_d(\vec{r},\nu)E^*_{ref}(\vec{r},\nu) + \text{c. c.}\}. \tag{2}$$

The same expression, without the frequency dependence, forms the basis of standard spatial holography. The interference terms at the right of Eq. 2 contain detailed information on the spectral and spatial behavior of the electric fields of the two incident beams. Data can be recalled (Fig. 1(b)) by illuminating the storage material with a read beam which is identical to the reference beam. The material now acts as a spatial-spectral filter. Immediately after passing through the material, the signal component of the transmitted read beam obeys the following proportionality[7]

$$E_s(\vec{r},t) \propto \int_{-\infty}^{\infty} E_{rd}(\vec{r},\nu)E^*_{ref}(\vec{r},\nu)E_d(\vec{r},\nu)e^{2\pi i\nu t}\, d\nu\ . \tag{3}$$

The expression for the signal beam (Eq. 3) contains the full richness of spatial holography along with the only partially explored capabilities (such as time-domain memory [8-17]) associated with the *spectrally-* selective character of the storage material. Depending on the properties of the three input fields, the signal field (Eq. 3) may duplicate the temporal waveform of one input field [8-17] or it may represent a variety of convolution/cross correlations of the input beam waveforms[18-21]. In the following, only the significant optical functionalities derived from Eq. 3 that have been explored as part of the completed project are described. It should be clearly pointed out that the results presented here only reveal only a small range of the potentially useful phenomena that can be realized through interaction of light with frequency-selective recording media.

Swept-Carrier Optical Memories

Swept-carrier frequency-selective optical memories[16,17,22,23] are one example of a technologically important functionality derived from the interaction of three optical beams with a frequency-selective recording material. The basic scheme of swept-carrier memory is depicted in Figure 2. During recording, two beams are simultaneously incident on the storage material. The optical carrier frequency of the beams may be offset by a

small amount and the carriers of both beams are "swept" across the spectral recording bandwidth of the storage material. The amplitude of the reference beam is held essentially constant, but the amplitude and/or phase of the data beam is modulated so as to encode data. Recording may be repeated at various spots across the surface of the storage material. To recall stored information, an read beam having properties identical to the reference beam is made incident on a storage location. The read beam creates a signal beam having the same temporal structure as the data beam. The stored data is thus recovered. The maximum serial data bandwidth that can be accomodated with swept-carrier storage/recall is limited primarily by support technologies and will be so constrained into the foreseeable future since process-limited bandwidths are extremely high, i. e. tens to hundreds of Gigabits/sec.

During the course of the completed project, swept-carrier storage and recall was demonstrated for the first time.[17] Within months of the first demonstration, it was further demonstrated that swept-carrier storage can provide areal data storage densities higher than possible with state-of-the-art traditional-technology optical or magnetic memories[23].

In the high density demonstration experiment of Ref. 23, the data and reference/read beams were focused with a crossing angle of 80 mrad into a 500-μm-thick slab of 0.5-atomic-percent Tm^{3+}:YAG. The laser was tuned within the inhomogeneously broadened absorption profile of the 793 nm, $^3H_6(1)\rightarrow{}^3H_4(1)$ transition of ^{3+}Tm to a frequency at which the slab's linear absorption is about 30%. The Tm^{3+}:YAG material was chosen because its transition wavelength falls within the tuning range of the commercial GaAlAs semiconductor diode lasers available for the experiment, rather than for its storage persistence. This material offers only about 10 msec of unrefreshed information storage time. Optical powers of reference/read and data beams were 1.0 mW and 1.4 mW, respectively, as they enter the sample. An Analog Module, Inc. 712A-4 APD (45 MHz bandwidth) avalanche photodiode - preamplifier combination was used for detection of memory output signals. Experiments conducted in the course of this project demonstrated

Swept-carrier time-domain frequency selective optical memory

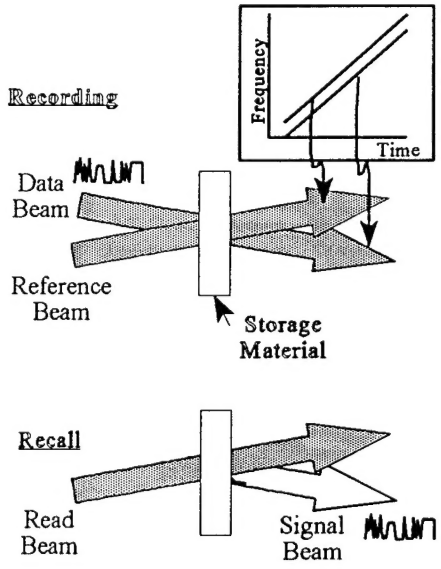

Figure 2. Swept-Carrier input and signal beams. Spatial, spectral and temporal behavior.

Thomas W. Mossberg, P. I.
Department of Physics
University of Oregon

for the first time the ease with which simple photodiode or avalanche photodiode based detection systems could be employed to detect spectral holographic signals.

Maximal areal density was achieved with the data and reference/read beams focussed to an elliptical spot size of 12x16 μm (intensity FWHM) in the storage crystal providing for a beam overlap length and beam confocal parameters comparable to the slab (refractive index ≈1.8) thickness. Amplitude modulation was employed to encode a 1760-bit long data sequence (80 repetitions of a 22-bit sequence with 6 bits high, bit duration of 50 nsec) onto the frequency-chirped (r_{CH} = 9.8 MHz/μs), 88-μsec-duration data beam. The frequency offset between data and reference beam, ν_{rd}, was 10 MHz. In determining areal density, the minimum beam cross sectional area was employed. This is appropriate since a displacement of the read beam by a minimum waist diameter should, through intensity and wavefront mismatch, suppress the output signal associated with the location.

The single-event storage and retrieval results shown in Figure 3 represent 8 Gbit/in^2 areal storage. The storage time was 200 μsec. Laser tuning constraints allowed for the use of only about ten percent of the available storage material bandwidth. Extrapolation of present results to full material utilization suggest an attainable density of nearly 100 Gbit/in^2. Note that this extrapolation is consistent with the process limits analyzed in Ref. 24.

In Figure 3, the signal beam power is about 10^{-5} of the data beam power. This value is substantially below the more optimal 10^{-2}-10^{-3} output/input power ratio one might expect in an unrelaxed, one-absorption-length thick, optimally excited storage material. The relative smallness of the output signal in the present experiment can be attributed to several factors including insufficient optical thickness, unoptimized excitation beam intensities, and sample relaxation. The latter effect turns out to be surprisingly important. It is found that instantaneous diffusion effects (excitation-induced frequency shifts of active absorber ions[25-28]) lead to large increases in the effective homogeneous linewidth in storage situations. The measured, 3.3 K, weak excitation, homogeneous linewidth, $\Delta\nu_h$, of about 40 KHz was found to increase to about 400 KHz under storage excitation conditions. With the excitation-beam chirp rate, r_{CH}, and spectral offset, ν_{rd}, experimentally employed, instantaneous diffusion reduces signal intensity in proportion to the factor $\exp[-4\pi\nu_{rd}\Delta\nu_h/r_{CH})] \approx 0.02$. Note that the signal beam duration in Figure 3 is about two orders of magnitude longer than instantaneous-

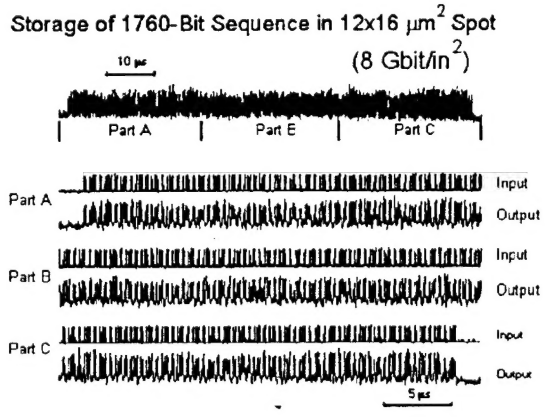

Figure 3. Data sequence stored using the swept-carrier technique at the areal density of 8 Gbit/in^2.

diffusion-shortened dephasing time of the storage material.

In other swept-carrier experiments, the storage of up to 4 Kbit of data at single spatial storage locations was demonstrated. When excitation-mediated dephasing is accounted for, one finds that the achieved spectral multiplicities were limited by the number of spectral channels available in the storage material within the frequency range utilized. The ability to store large numbers of data bits at single spatial locations is important because changing spatial addresses tends to be slow. Using high bandwidth recording/recall of long data strings at single spatial locations may open the possibility of entirely new memory architectures. For example, Gigabit/sec spectral holographic memories may provide a much higher speed and density alternative to dynamic RAM

Heterodyne detection of Swept-Carrier Signals

Swept-carrier output signals are cotemporal, spectrally offset, and typically two or more orders of magnitude smaller than the read beam. In the experiments described above, input beam angling was utilized to create output signals that are directly detectable by virtue of their distinct output direction. Beam angling adds complexity to the necessary optical apparatus and is therefore undesirable. When storage is effected with collinear data and reference beams (providing for a simple optical apparatus), the read and signal beams are also collinear implying that direct detection of the signal beam is not possible. However, because of the frequency offset between the read and signal beams, a heterodyne beat signal is expected in the combined read+signal intensity. As part of this funded project, it was experimentally demonstrated[22] that the heterodyne signal just described provides an accurate representation of stored data, provides sufficient amplification of signal level to permit signal detection with simple non-avalanche Si photodiodes, and simplifies the basic optical setup required by eliminating the need for multiple, non-collinear but intersecting, optical beams and/or optical shutters. In Figure 4, a series of traces representing the heterodyne detection and demodulation of a swept-carrier memory signal produced with collinear input beams is presented. In Figure 5, the extremely simple experimental apparatus that can be employed in the case of collinear input beams is shown. The simplicity with which the swept-carrier signals can be detected, is an important positive attribute in terms of the prospective technological application of the process.

Optical Bit Rate Conversion

It was successfully demonstrated[30] that the swept-carrier approach to data storage can be implemented so as to allow for optical bit-rate conversion and bit-stream time reversal. These functions may serve to facilitate the reception, transmission, and processing of data falling outside normally acceptable bandwidths.

Bit-rate conversion/bit-stream time reversal is effected, as in the case of memory,

Thomas W. Mossberg, P. I.
Department of Physics
University of Oregon

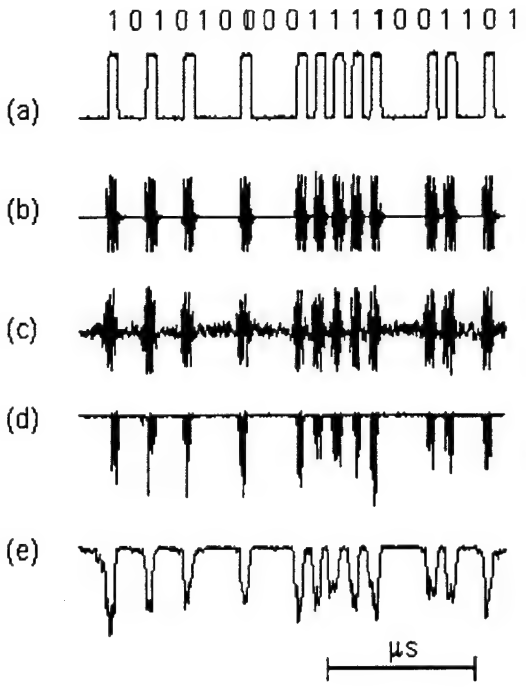

Figure 4. (a) Data Beam; (b) Heterodyne between data and reference beams; (c) Heterodyne between read and signal beams; (d) Trace c rectified; (e) Trace d, low-pass filtered.

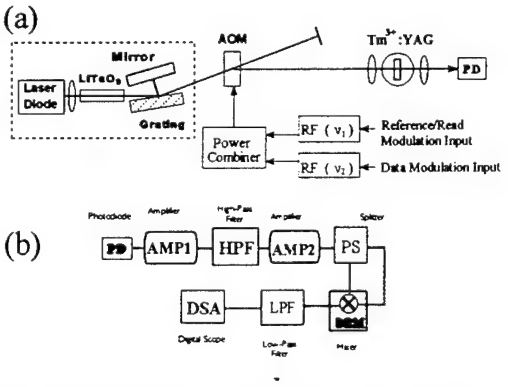

Figure 5. (a) Swept-carrier apparatus using heterodyne detection. (b) Heterodyne demodulation electronics.

through the interaction of three distinct optical beams with a frequency-selective storage material. The first two beams, the reference and data beams, interact with the storage material, modify its absorption profile, and create spatial gratings to deflect the signal beam in a specific output direction. The third beam, the read beam, induces the storage material to emit a signal beam. In the case of interest here, the signal beam consists of a copy or a modified copy (time-reversed, altered bit rate) of the data beam. The input beams each consist of an optical carrier that is frequency chirped at a rate R_ϵ. It is assumed throughout that $R_{ref} = R_{data}$ and that all three beams are chirped over the same bandwidth B. The input beams have constant envelope except for the data beam which is modulated to encode a data stream.

The parameter $\eta \equiv |R_{data}|\tau_{db}^2$, where τ_{db} is the duration of individual bits within the data beam, is important. For $\eta > 1$ (the data beam chirps more than a bit bandwidth per bit duration), data bits can be assigned to unique spectral positions. For $\eta < 1$, bits are spectrally intermixed. When the chirp rates of reference/data and read beams are identical, the signal beam reproduces the data beam waveform exactly regardless of the value of η. This result leads, in memory applications, to the ability to store many bits per τ_{db}^{-1} bandwidth.

More generally, the magnitude and even the sign of the read-beam chirp rate may differ from the reference and data beams. If $\eta \geq 1$ and $\eta/|\Re| \geq 1$, where $\Re = R_{read}/R_{ref}$, the data-beam bit sequence will still be reproduced in the signal beam, but the bit-sequence will be temporally expanded

Thomas W. Mossberg, P. I.
Department of Physics
University of Oregon

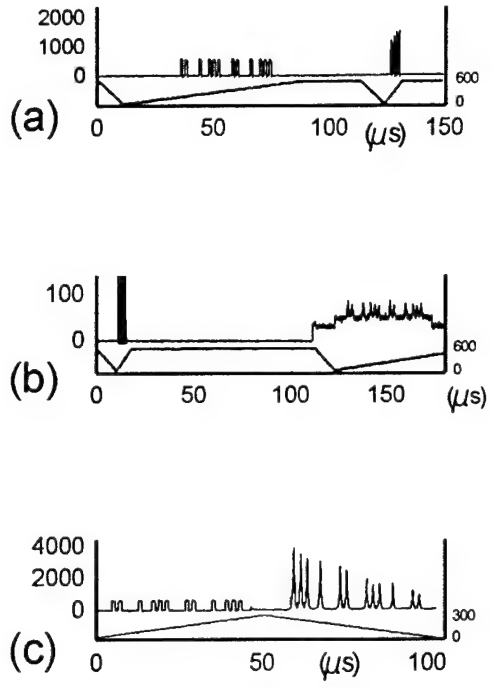

Figure 6. Optical bit-rate conversion

(compressed) for $|\Re|<1$ ($|\Re|>1$) and time-forward (time-reversed) for $\Re>0$ ($\Re<0$). The signal-beam and data-beam bit rates, ρ_{sig} and ρ_{data}, respectively, are related according to $\rho_{sig}=\rho_{data}|\Re|$. As the conditions $\eta\geq 1$ and $\eta/|\Re|\geq 1$ are less well satisfied, the temporal profile of the signal beam will become less well correlated with that of the data beam (unless $\Re\approx 1$).

Fig. 6 shows actual experimental recordings of bit-rate modification and time-reversal. The optical intensity measurement shown in the upper full trace of each plot represents the output of a detector looking along the signal direction. The left-hand portion of each top trace records a small portion of the data beam scattered in the signal direction, while the right hand portion represents the direct signal beam. The measured carrier frequency of the ref (read) beam is shown at the left (right) of the lower trace in each plot. Fig. 6(a) shows a situation where $\Re = 10$ so that the signal beam is only 0.1 times as long as the data beam. The signal beam bit rate is thus ten times that of the data beam. While acquiring this data ν_{RD}= -0.5 MHz, R_{ref} (R_{read}) was 8(80) MHz/μs, and τ_{db} was 1.0 μs. Here η=8 and $\eta/|\Re|$=0.8. Although $\eta/|\Re|$ is slightly smaller than unity, it is found that the signal beam is a faithful bit-rate-shifted copy of the data beam. The output signal power here is about 2×10^{-5} of that of data beam. In Fig. 6(b), R_{ref} (R_{read}) was 80(8) MHz/μs, τ_{db} =0.1 μs, ν_{RD}= -5 MHz, and $\Re$ = 0.1. In this case η=0.8 and $\eta/|\Re|$=8. Again it is found that the output signal is a faithful copy of the data beam with a ten times smaller bit rate. Note that all upper traces in Fig. 6 have the same vertical scale of signal size. Fig. 6(c), shows bit stream time reversal ($\Re$ = -1) with R_{ref} (R_{read}) = 6.4 (- 6.4) MHz/μs, τ_{db} = 1 μs, ν_{RD} = - 4 MHz, η=6.4, and $\eta/|\Re|$=6.4. As predicted, the output signal (right side top trace) is a time-reversed duplicate of the input data beam (left side top trace). Other negative values of $\Re$ should be acceptable and provide time reversal and bit rate modification. The damping effect seen in Fig. 6(c) is caused by excitation-induced relaxation within the storage material[25-29] and is manifest most strongly in instances involving time reversal. The effect of this dephasing on a given bit is proportional to the number of atoms excited between the bit's storage and retrieval. In cases of time reversal, the early input bits are maximally affected

by this dephasing. In time forward implementations, all bits are affected equally (to a first approximation). The dephasing observed is dependent on the detailed excitation conditions and the particular storage material employed. The effects of excitation-induced dephasing can be minimized by suitable choices of operational parameters.

Temporal-Waveform-Controlled Spatial Routing of Optical Beams

As part of the funded research, a scheme for the routing of optical data beams utilizing both spatial and spectral holographic functionality has been devised.[31] In this process, optical signals propagating along a common direction are routed into different and distinct output directions according to the precise temporal waveform encoded onto each signal, i. e. the routing function is controlled by the temporal structure of input signals. The routing is passive and expected to be implementable with subpicosecond or longer input signals. One can envision a number of applications. As an optical data router, for example, input signals, each encoded with a temporal address code, are passively directed into a destination direction and simultaneously stripped of their temporal encoding pattern.

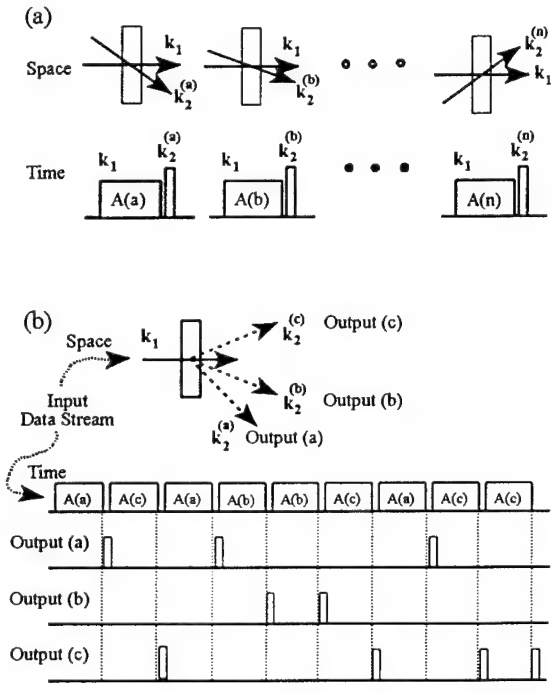

Figure 7. Temporal-Waveform-Controlled Spatial Routing of Optical Beams. (a) Programming; (b) Operation.

Temporal waveform-controlled spatial routing of optical beams has two distinct stages. The first stage is referred to as the programming stage. Programming may be accomplished in a variety of ways. In the present instance, programming is accomplished through exposure of the frequency-selective recording material to one pair of programming pulses for each output direction desired (see Figure 7). A given programming pulse pair consists of an address programming pulse, $E_a(r, t)$, and a direction programming pulse, $E_d(r, t)$. These two pulses are temporally sequential with the address pulse first. All address programming pulses propagate in the same direction k_1, but each such pulse is encoded with a unique temporal waveform. The direction programming pulses propagate in different directions and define the output directions of the router. Input optical signals will be processed and deflected along the output direction associated with a certain programming pulse pair if the temporal

waveforms of the input and corresponding address programming pulse are identical.

In the operational stage, the programmed material is illuminated by a data stream consisting of temporally structured optical pulses. The data beam propogates along k_1 (same direction as the address programming beams) and has the electric field $E_{data}(r, t)$. In the presence of the data beam, the pre-programmed recording material will emit signals in all programmed directions. These signals can be written as a sum, with each term corresponding to the signal emitted in a specific programmed direction, i. e.

$$E_{sig}(r,t) = \sum_{(i)} \int_{-\infty}^{+\infty} E_a^{(i)^*}(\nu)\, E_d^{(i)}(\nu)\, E_{data}(\nu) \times e^{2\pi i \nu (t - r k_2^{(i)}/c)}\, d\nu \qquad (4)$$

where $E_{data}(\nu)$ is the Fourier transform of the input data beam and (i) represents different programming pulse pairs. Assuming that the direction beam, $E_d^{(i)}(t)$, is temporally brief for all (i), the deflected beam in direction $k_2^{(i)}$ will be large only when the address beam, $E_a^{(i)}(t)$, is identical to a segment of the data beam, $E_{data}(t)$.

A preliminary experimental study of the routing function (see Fig. 8) was conducted in the course of the funded research. In this experiment, optical signals incident along one direction (Address/Data Beam direction) are deflected into one of two output directions (defined by Direction Beams A and B). An external-cavity-stabilized diode laser system and three acousto-optic modulators (AOM's) are used to produce all the optical beams. AOM1 and AOM3 produce direction programming beams A and B, respectively. AOM2 produces the address programming beams as well as the subsequent input data beam. All beams have an optical power of about 1 mW, are focused on the routing material with the minimum spot diameter of about 30 μm. The frequency-selective material employed consists of Tm^{3+}:YAG which is cooled to ≈3.2 K. The diode laser is tuned to the $^3H_6(1) \rightarrow {}^3H_4(1)$ transition of Tm^{3+} at 793 nm. Adjacent beams shown in Fig. 8 cross at an angle of ≈ 40 mrad. Output signals emitted along directions A and B are detected using silicon avalanche photodiodes.

Figure 9(a-c), shows the temporal sequence of electrical signals used to drive a balanced mixer controlling the AOM drive fields during router programming. Traces (a)-(c) correspond, respectively, to AOM2, AOM1, and AOM3. The bipolar character of trace (a)

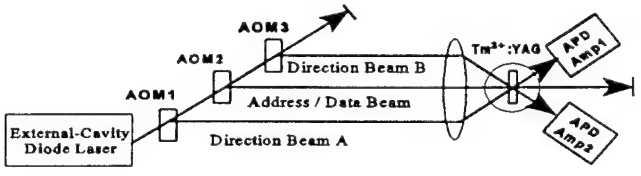

Figure 8. Waveform-controlled spatial routing experimental schematic.

Thomas W. Mossberg, P. I.
Department of Physics
University of Oregon

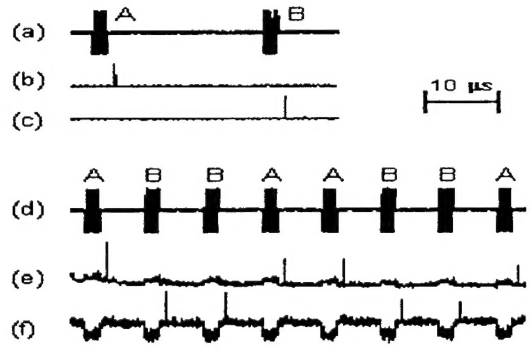

Figure 9

represents binary ($\pm\pi$) phase modulation which was used to structure the address programming pulses. Address pulses for the two directions programmed consist of different 20-bit binary phase codes. Figure 9(d) shows the electrical signal used to generate the data beam. Figures 9(e) and 9(f) correspond to the same time window as trace (d) and are recordings of light intensity directed by the router into directions A and B, respectively. The narrow peaks constitute the primary signal. Note that the long data beam pulses are temporally compressed and demodulated as they are deflected. The level changes in traces (e) and (f) that occur simultaneously with the pulses of trace (d) represent changes in leakage into the output directions introduced by the operation of AOM2. It is clear that cross talk between the channels is small. The principles demonstrated in this first experiment, have substantial potential technologically. For very high speed operation, frequency-selectivity needed becomes courser and storage materials employed will be operable at substantially higher temperatures - perhaps as high as room temperature.

Summary

Over the last three years, a very preliminary but extremely successful program focussed on the theoretical and experimental elucidation of spatial-spectral holography has been completed. Areal storage densities and density-bandwidth products substantially beyond those reported for traditional magnetic or optical memory have been demonstrated. Achievement of such high performance so very early on in the development of the technology provides an inkling of the inherent technological potential of spectral and combined spatial-spectral holographic processes. A variety of new functionalities beyond memory have been discovered and demonstrated. Additional developments associated with spatial-spectral holography, both evolutionary and revolutionary, can be expected in the future.

References

1. A. Szabo, U. S. Patent 3,896,420 (July 22, 1975)
2. G. Castro, D. Haarer, R. M. Macfarlane, and H. P. Trommsdorff, U. S. Patent 4,101,976 (July 18, 1978).
3. W. E. Moerner, J. Mol. Electron. **1**, 55 (1985).
4. W. E. Moerner, Persistent Spectral Holeburning: Science and Applications (Springer-

Verlag, Berlin, 1988).
5. A. Renn, A. J. Meizner, U. P. Wild, and F. A. Burkhalter, Chem. Phys. **93**, 157 (1985).
6. U. P. Wild and A. Renn, J. Mol. Electron. **7**, 1 (1991).
7. T. W. Mossberg, Opt. Lett. **7**, 77 (1982).
8. Y. S. Bai, W. R. Babbitt, and T. W. Mossberg, Opt. Lett. **11**, 724 (1986).
9. J. M. Zhang, D. J. Gauthier, J. Huang, and T. W. Mossberg, Opt. Lett. **16**, 103 (1991).
10. W. R. Babbitt and T. W. Mossberg, Opt. Commun. **65**, 185 (1988).
11. M. K. Kim and R. Kachru, Opt. Lett. **14**, 423 (1989).
12. M. Mitsunaga and N. Uesugi, Opt. Lett. **15**, 195 (1990).
13. M. Mitsunaga, R. Yano, and N. Uesugi, Opt. Lett. **16**, 1890 (1991).
14. X. A. Shen and R. Kachru, Opt. Lett. **18**, 1967 (1993).
15. Y. Bai and R. Kachru, Opt. Lett. **18**, 1189 (1993).
16. T. W. Mossberg, Opt. Lett. **17**, 535 (1992).
17. H. Lin, T. Wang, G. A. Wilson, and T. W. Mossberg, Opt. Lett. **20**, 91 (1995).
18. Y. S. Bai, W. R. Babbitt, N. W. Carlson, and T. W. Mossberg, Appl. Phys. Lett. **45**, 714 (1984).
19. W. R. Babbitt and J. A. Bell, Appl. Opt. **33**, 1538 (1994); U. S. Patent 5,239,548.
20. M. Zhu, W. R. Babbitt, C. M. Jefferson, submitted to Optics Letters.
21. K. D. Merkel and W. R. Babbitt, submitted to Appl. Optics.
22. H. Lin, T. Wang, G. A. Wilson, and T. W. Mossberg, Opt. Lett. **20**, 928 (1995).
23. H. Lin, T. Wang, and T. W. Mossberg, Opt. Lett. **20**, 1658 (1995).
24. W. R. Babbitt and T. W. Mossberg, J. Opt. Soc. Am. B **11**, 1948 (1994).
25. J. Huang, J. Zhang, A. Lezama, and T. W. Mossberg, Phys. Rev. Lett. **63**, 78 (1989), J. Huang, J. Zhang, and A. Lezama, Opt. Commun. **75**, 29 (1990).
26. G. K. Liu and R. L. Cone, Phys. Rev. B **41**, 6193 (1990).
27. M. Mitsunaga, T. Takagahara, R. Yano, and N. Uesugi, Phys. Rev. Lett. **68**, 3216 (1992).
28. Y. S. Bai and R. Kachru, Phys. Rev. B **46**, 13735 (1992).
29. S. Kroll, E. Y. Xu, and R. Kachru, Phys. Rev. B **44**, 30 (1991).
30. T. Wang, H. Lin, and T. W. Mossberg, Opt. Lett. (to appear Oct. 1995).
31. W. R. Babbitt and T. W. Mossberg, Opt. Lett. **20**, 910 (1995).
32. Yu. T. Mazurenko, Appl. Phys. B **50**, 101 (1990).
33. E. L. Hahn, N. S. Shiren, and S. L. McCall, Phys. Lett. **37A**, 265 (1971).

Articles Published under AFOSR support:

1. Quasi-two-dimensional time-domain color memories: Process potentials and limitations, T. W. Mossberg and W. R. Babbitt, J. Opt. Soc. Am. B **11**, 1948 (1994).

2. Experimental Demonstration of Swept-Carrier Time-Domain Optical Memory, H. Lin, T. Wang, G. A. Wilson, and T. W. Mossberg, Opt. Lett. **20**, 91 (1995).

3. Spatial Routing of optical beams through Time-Domain Spatial-Spectral Filtering, W. R. Babbitt and T. W. Mossberg, Opt. Lett. **20**, 910 (1995).

4. Heterodyne Detection of Swept-Carrier Time-Domain Memory Signals, H. Lin, T. Wang, G. Wilson, and T. W. Mossberg, Opt. Lett. **20**, 928 (1995).

5. Demonstration of 8 Gbit/in^2 areal storage density using swept-carrier frequency-selective optical memory, H. Lin, T. Wang, and T. W. Mossberg, Opt. Lett. **20**, 1658 (1995).

6. Optical Bit Rate Conversion and Bit Stream Time-Reversal Using Swept-Carrier Frequency-Selective Optical Data Storage Techniques, T. Wang, H. Lin, and T. W. Mossberg, Opt. Lett. (accepted for publication).

7. Experimental Demonstration of Temporal-Waveform-Controlled Spatial Routing of Optical Beams via Spatial-Spectral Filtering, Opt. Lett. (accepted for publication).

8. Frequency Agile Narrow Linewidth Semiconductor Diode Laser System, H. Lin, T. Wang, A. Sutton, and T. W. Mossberg (in preparation).

Personnel and Degrees Granted

Dr. Geoffrey Wilson - Post Doctoral Research Associate
Mr. Hai Lin - Graduate Research Assistant (Ph.D. expected late 1995)
Mr. Tsaipei Wang - Graduate Research Assistant (Ph.D. expected late 1996)
Mr. Christoph Greiner - Graduate Research Assistant
Ms. Amy Sutton - Summer Undergraduate Research Assistant
Prof. Thomas Mossberg - Principal Investigator

Patents

U. S. Patent Number 4,459,682. Time-domain frequency-selective optical memories. Issued July 10, 1984.

Temporally Programmed Spatial Routing of Optical Beams, Patent Pending.